www.czasopisma.pan.pl PAN www.journals.pan.pl

ARCHIVES of FOUNDRY ENGINEERING

ISSN (2299-2944)

10.24425/afe.2024.151313

Published quarterly as the organ of the Foundry Commission of the Polish Academy of Sciences

Ultrasonic Crystallization of Monotectic Zn-2%Bi Alloy

A. Szot, G. Boczkal *, P. Pałka
AGH University of Science and Technology, Poland
* Corresponding author: E-mail: gboczkal@agh.edu.pl

Received 05.09.2024; accepted in revised form 22.10.2024; available online 24.12.2024

Abstract

In current studies, the authors examined the influence of ultrasonic vibrations on the solidification of Zn – Bi 2% alloy. The research reveals that ultrasonic vibrations have a sufficient influence on the crystallization process. In the case of both groups of ingots (Zn and Zn-2%Bi), the differences in microstructure and mechanical properties could be observed. The methodology was based on the casting of two samples from the same ingot form with identical configurations. One of the samples was used as the reference (cast without ultrasonic) and the other to examine ultrasonic vibrations' influence. Casting with ultrasonic vibration was carried out with a frequency of 35 kHz. Sonotrode was located on the underside of the designed crucible. The samples were circular shape with a diameter of 50 mm and a thickness of 10 mm. A tensile compression test, Vickers microhardness test and microscopy analysis were performed. The results showed enhanced organization of microstructure and the fragmentation of grains in the case of the ingots with the ultrasonic vibration presence.

Keywords: Monotectic alloys, Ultrasonic casting, Non-equilibrium crystallization

1. Introduction

One of the oldest and most common methods of manufacturing alloys is casting. Over the past centuries, it has been developed and optimized. The most popular casting methods are permanent pattern casting, temporary pattern casting, die casting, centrifugal casting, squeeze casting, and continuous casting [1]. Depending on the method, the properties of the casted material could be different. This phenomenon is mainly due to the solidification process of materials. The crystallization process is based on two mechanisms, nucleation and growth. The nucleation process can be classified as homogeneous nucleation and heterogeneous nucleation [2]. Compared to homogeneous nucleation, the energy required to start the heterogeneous nucleation is lower [3]. The crystallization process and its parameters, such as the cooling rate, temperature gradient, and others, influence the shape and size of the grain. Control of the process by factors such as temperature, heat provided into the system, speed and directions of thermal energy dissipation, distribution of seed density in a matrix, time of seed creation, growth of crystalline layers, strain induced within the system and direction of foreign particles in the system allows providing needed crystallographic structure [4 – 6].

One of the methods that allowed microstructure control in casted alloys are ultrasonic vibrations introduced during the crystallization process. The impact point of ultrasonic vibration on liquid metal can occur by several stages of casting:

- during input of a mold into a crucible by vibrating a stream of cast metal through a vibrating element in its path;
- by insertion of a vibrating element into the mold before it is flooded;
- use of the vibration at an entire casting system that mold contains a liquid alloy.

Depending on the stage in which the ultrasonic is introduced, the effect on the mold is different. As an example, the use of vibration at the casting form is to limit the defects in the fillings of the mold rims of the casting form. Regarding ultrasonic vibrations, factors such as frequency, power, distance from the source of

ultrasonic vibrations, the transmitter of ultrasonic, the size of the ultrasonic transmitter, time of material, and ultrasonic interaction are the most important to control their effect on the material structure.

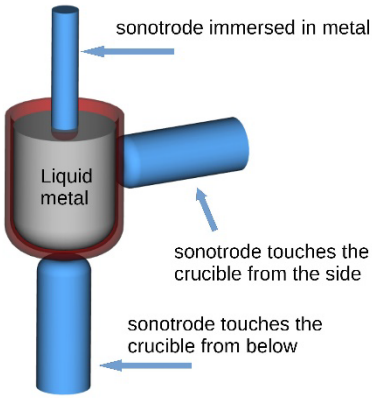

Fig. 1. Scheme of the input point of sonotrode in the casting process based on the description in the literature [6–10].

Although many authors tested the use of ultrasonic in eutectic systems, there is less information about ultrasonic effects on monotectic systems. In eutectic systems, the influence of ultrasonic vibration on a material structure is undeniable. Compering molds with and without ultrasonics vibrations, researchers inform about different mechanical properties (the value could differ even by 126 MPa), the finest structure of grains (depending on the casting stage in which the ultrasonic is introduced), modifying the structure of separation additions (finer the dendrites or replacing the shape to fine and equiaxed grain) and fewer pores in the mold without increasing the processing time [6–11]. Some researchers explored monotectic systems to solve the problem of segregation and agglomeration of other phases in an alloy. The first attempt to resolve the problem of monotectic phase agglomeration was a mechanical vibration with a small amplitude. As a result, casted ingots are characterized by a better distribution of monotectic phase and finer precipitation [12–14]. It must be noted that in both cases (eutectic and monotectic alloys), most of the research uses a low-frequency vibration in a range of 5 Hz to 100 Hz.

2. Methods

In this article, the authors decided to examine one of the monotectic binary systems, Zn – Bi. The research was motivated by an interest in the examination of the influence of ultrasound on the nucleation process during the crystallization of monotectic alloys. Because of a decrease in temperature, the two phases of the alloy are gravity segregated by different densities of phases in a liquid state. In the case of monotectic alloys, the ultrasonic vibrations should have disrupted the natural low-range order of the coexisting reaction with the solidification process. The first stage of crystallization is the creation of close-range segregation in both liquids. As a consequence, a seed of a new phase is created in the solid phase. The interference of ultrasonic vibration in liquid imposes limitations on the atom-order configuration. This leads to the precipitation of seeds from the solid phase. The implementation of ultrasonic vibrations in the liquid phase reduces the possibility of close-range segregation in the liquid. As a result, the crystallization process goes without primary precipitations. As an effect, structural changes such as fining the grains and the growth of grains by heat dissipation in microstructure can be observed.

3. Experiments

3.1 Casting

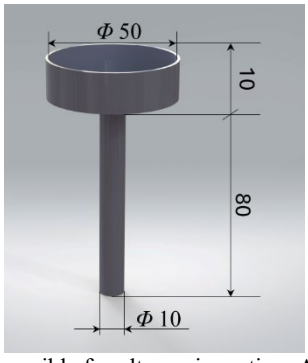

Fig. 2. Model of crucible for ultrasonic casting. A cast station was prepared for the comparison section.

The crucible was designed to include factors such as the size of the casting material, the frequency of the ultrasonic source, the crucible material (stainless steel), and the distance of the crucible from the source [15]. Two designed forms (Figure 2) were cleaned with ethanol and then rinsed up with water. Crucibles were placed next to each other, and 4 ingots were prepared (2 for each alloy with and without ultrasonic treatment) for the ultrasonic source (35 kHz). Ingot I: 279.79 g of Zn (99.997%) (Goodfellow 289-548-84), Ingot II: 274.19 g of Zn (99.997%) (Goodfellow 289-548-84) + 5.595 g of 99.999% Bi (Sigma-Aldrich 556130)

After the temperature reached 500°C, ingots were put into the crucible and left in the furnace for 30 min. The melted samples were cast on the cold forms. Casted samples were left freely with the assistance of ultrasonic vibration until the crystallization process was fully done (c.a. 3 min). The samples were cooled in a stream of cooled water for 2 min.

3.2 Preparation of the casted sample for macroscope/microscope and mechanical analysis

In the case of Zn samples, the upper surface was grinding and polished on wet cotton fabric using $CuCl_2$ supersaturated saline solution with a base of 2% nital and then cleaned with a paste made of supersaturated saline solution citric acid. For microscopy analysis, Zn – Bi 2% samples were etched and electropolished (in

the range of 5 V – 10 V, polishing for 5 min in 10 V, 8V, 5V) by a mixture of H_3PO_4 and ethanol (proportion 3:5, for 7 min in 0.7 V). The prepared samples were taken under macroscope and microscope analysis (Electron Scanning Microscope Hitachi S3400N (Hitachi High-Tech Corporation, Japan), Vert.A1 Zeiss Optical Microscope equipped with the Axiocam 305 color (Carl Zeiss AG, Germany). Next, the samples were cut perpendicular to the face surface to examine the cross-section part. The preparation of the surface was done in the same way as the face surface. Preparation of the samples for the compressive test was cut out by using a CNC machine BP05d Electrical Discharge Cutting Machine (Zakład Automatyki Przemysłowej B.P. s.c., Poland). The cutting was taken empirically by observation of the material during material cutting. Each of the sample models was cut in the schape of a cuboid (dimensions: 4x4x8 mm, ± 0.1). Then the compressive test was performed with a strain rate of 0.003 s^{-1}. The cut was taken from the center to the border of the sample. Tensile tests were performed on modified Instron TM-SM model 1112 tensile strength machine (Instron US) with 5kN load cell.

4. Results and discussion

The macrostructure of the Zn sample without the presence of ultrasonic vibrations are dominated by large and long columnar grains, directly solidified in the center of the sample. An exception is the frozen crystal ring around the sample, with fine grains (Figure 3a). The multiple columnar grains with twins directly crossed with each other can be seen (Figure 3c). The ingot has a large number of pores (Figure 3e). Different types of macrostructure can be observed for the ultrasonic vibration sample (Figure 3b, d, f). The presence of ultrasonic vibrations strongly influences the macrostructure of the Zn sample. Compared to the sample without ultrasonic vibrations (Figure 3a, c, e), the grains are shorter and thinner at the center of the sample (Figure 3b). Although the ring around the sample is also present as in the sample without the presence of ultrasonic vibrations, the macrostructure is much finer. The ingot is severely twined in various directions (Figure 3d). The sample is characterized by thinner and fewer pores (Figure 3f) than in the gravity casting (Figure 3e). It is worth noting that "the cracks" (black marks at the upper left side of Figure 3a) present in the sample appeared before etching and became more visible after it. The macrostructure of Zn samples without the presence of ultrasonic vibrations (Figure 4a) has no homogeneous structure. The sides of the sample have long, slim grains directed into the center of the sample, while the center of the sample has fine grains placed closer to its surface and substrate. In the case of the sample with ultrasonic vibrations (Figure 4b), the sample also has thicker grains. The exception is the center area of the sample where the grains are smaller. Although the samples have similarities, in the case of the Zn sample with ultrasonic vibrations (Figure 4b), the symmetry in the sample could be observed. The structure of the Zn sample is characteristic of the ingots cast gravitating. The structure has large, long, columnar grains directed at thermal dissipation.

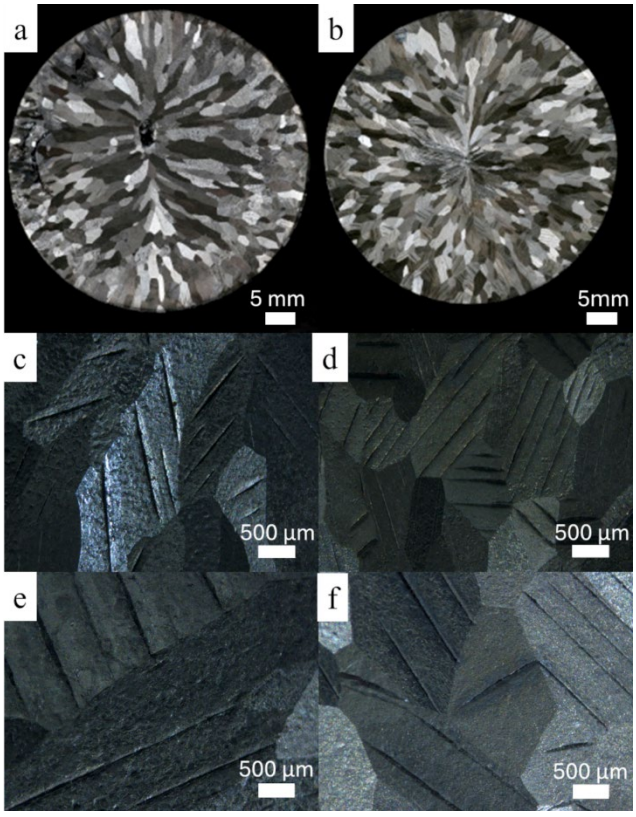

Fig. 3. Macrostructure of the cross-section of the Zn without the presence of ultrasonic vibrations (a, c, e) and Zn with the presence of ultrasonic vibrations (b, d, f).

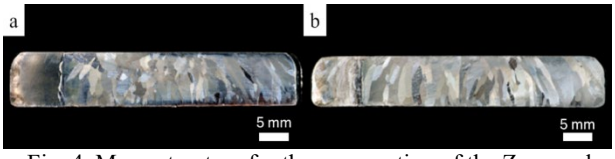

Fig. 4. Macrostructure for the crosssection of the Zn samples, a) Zn – without the presence of ultrasonic vibrations, b) Zn with the presence of ultrasonic vibrations.

Based on the data from the compression test, it can be said that the mechanical properties of the ingot are not unified. Inverse properties are being observed for the Zn sample with the ultrasonic vibrations. Compared to the sample without ultrasonic vibrations, the microstructure of the ingot has a symmetrical distribution of the grains both on the face surface and cross-section of the ingot (Figure 3 and Figure 4). Additionally, the grains are equiaxed, finer, and are more evenly distributed on the surface of the ingot. The result for the sample with ultrasonic vibrations shows similarity in mechanical parameters, however, the strengthening factor measured in the plastic range is higher about 2.6. This indicates that the ultrasonic vibrations made the sample homogeneous.

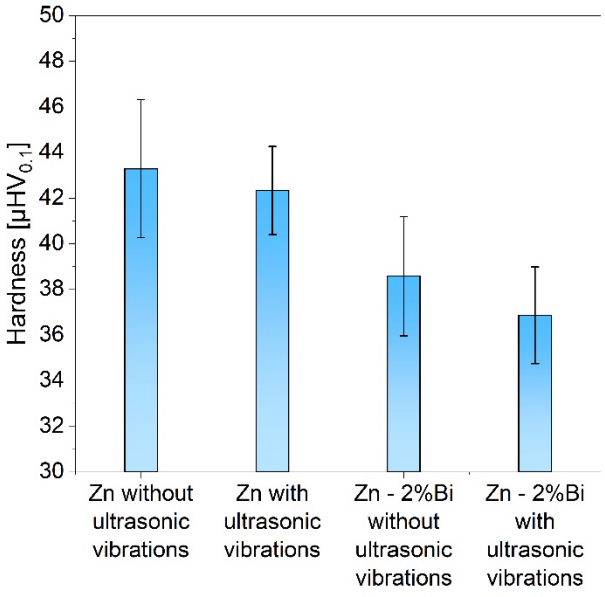

Fig. 5. Diagram of hardness for Zn and Zn – 2%Bi samples.

The hardness measurements (Figure 5) reveal that samples cast with the presence of ultrasonic vibrations has lower standard deviations than the sample without it. As a result, the structure of the sample with ultrasonic vibrations has a lower hardness average than the other one. This phenomenon is connected with the unification of structure and phase distribution by ultrasonic vibration. In the case of Zn samples, the standard deviations fall from 3 to 1.9, and for the Zn – 2%Bi from 2.6 to 2.1. A similar position of the sonotrode and observations were made for the Al – Si 10Mg alloy by P. Karthikeyan and Sumit Pramanik [16, 17]. However, the authors pointed out that in their case, the important factor in obtaining the finest structure is the time of ultrasonic vibration use. In this work, the ultrasonic vibrations are continuous until the full solidification of an ingot. The time aspect of its use was also highlighted by Hélder Puga et al. as a resolution of pores in ingot [8]. In the case of the sample without ultrasonic vibrations (Figure 6c), the distribution of the grains is nonunified. In the case of the sample with ultrasonic vibrations, the distribution of the grains is more equal and appears to be independent of the distance from the center. A slight increase is noted in the direction of the edge of the sample. The data (Figure 6d) show that the dominant grain size fraction for the sample without ultrasonic vibrations is 4 – 32 mm and 32 – 60 mm. The percentage of bigger grains equals 17 %. For the sample with ultrasonic vibrations, the main size fractions that are almost equal to each other are grains in a range of 4 – 58 mm and 32 – 60 mm. The percentage of bigger grains is 14 %.

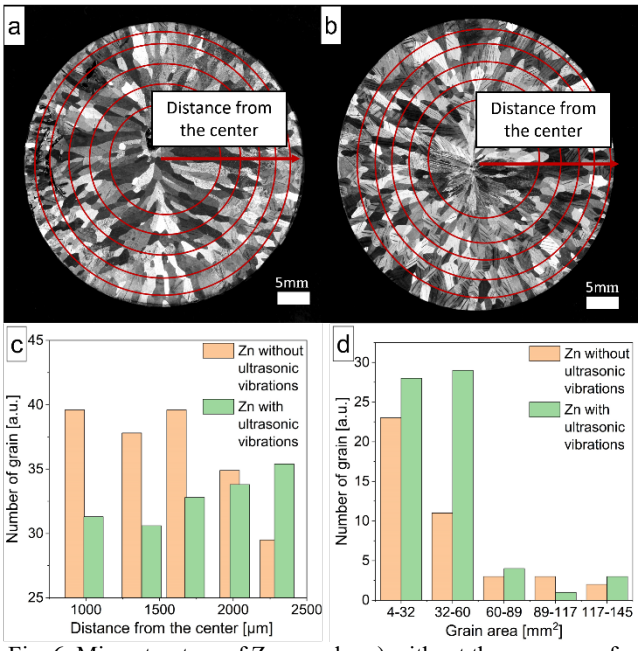

Fig. 6. Microstructure of Zn samples a) without the presence of ultrasonic vibrations and b) with the presence of ultrasonic vibrations 35 kHz. Red circle frames are for statistics (Figure 6c), d) diagram of grain size distribution.

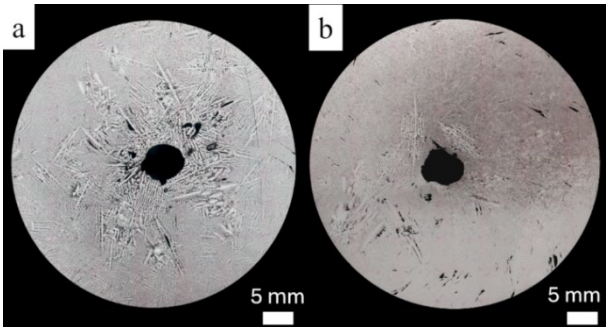

Fig. 7. Macrostructure for the Zn – 2% Bi samples, a) Zn – 2% Bi – without the presence of ultrasonic vibrations, b) Zn – 2% Bi with the presence of ultrasonic vibrations.

The microstructure (Figure 7a) is characterized by large dendrites at the entire area of the face surface accumulated in the center of the ingot, that thoroughly surrounds the casting pit. Although in the case of the sample with the presence of ultrasonic vibrations (Figure 7b), the dendrites are also present, they are smaller. The area around the casting pit has only a few large dendrites. In the casting of Zn – Bi 2% ingot in the presence of ultrasonic vibrations, there are cracks in the material. It is opposite to the Zn system, where the presence of cracks in the ingot was noticed without the presence of ultrasonic vibrations.

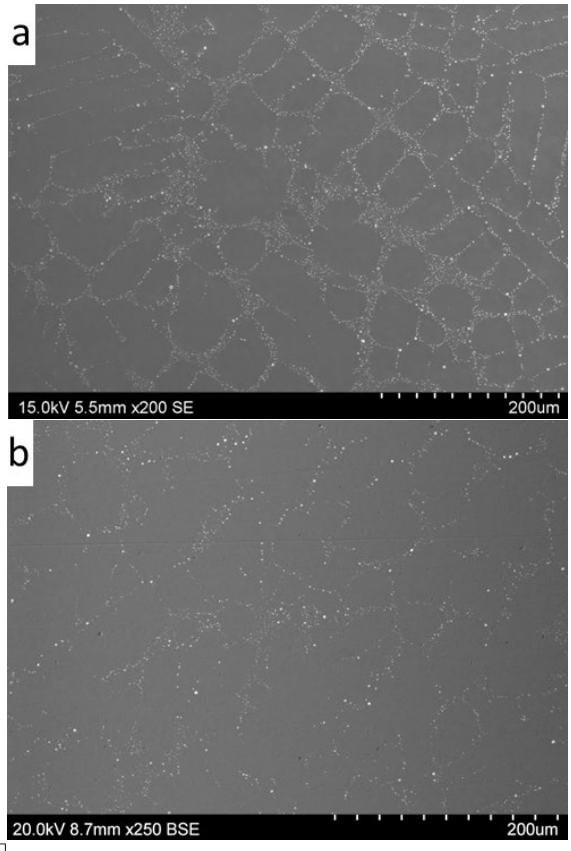

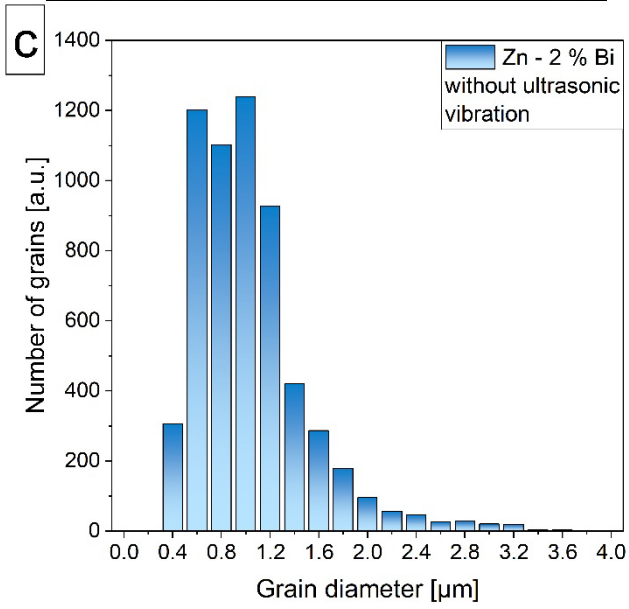

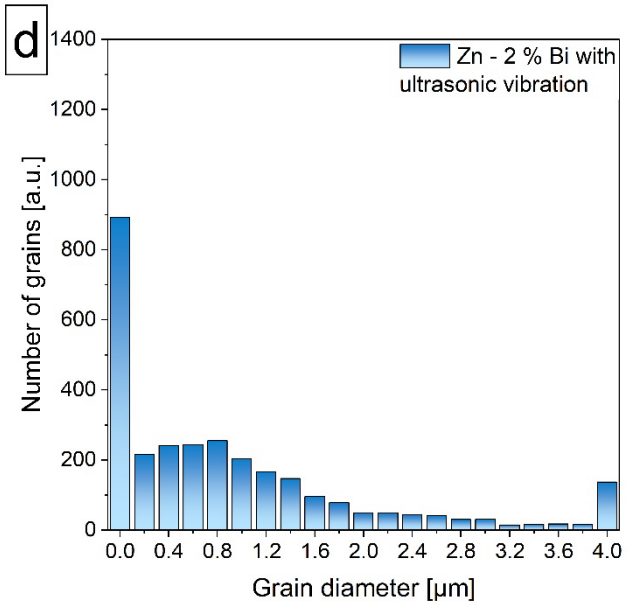

Fig. 8. SEM photography of Zn – 2% Bi – without the presence of ultrasonic vibrations a), with the presence of ultrasonic vibrations b), the statistic diagram of the grain diameter for the sample without ultrasonic vibrations c), with ultrasonic vibrations d). The grain diameter was calculated with the Matlab algorithm.

The SEM photography of Zn – 2% Bi without ultrasonic vibrations (Figure 8a) shows that the structure is non-uniform and characterized by large dendrites. The accumulation of fine bismuth participations is located along the arm of the dendrites, leaving space between the arms. In the case of Zn – 2% Bi sample (Figure 8b) with the presence of ultrasonic vibrations, the distribution of Bi – phase in the Zn matrix is high. As in the sample without the ultrasonic vibrations, the dendrites are also present. However, the ultrasonic vibrations sample does not have empty spaces between dendrites. The Bi – phases are not segregated in a specific direction. Based on the microscope image (Figure 8a, 8b), the histogram of the size of the bismuth phases was made. Histogram of the sample without ultrasonic vibrations Zn – 2% Bi (Figure 8c) shows a diversity of diameter size with the predominant amount of grains size diameter 0.6 to 1.4 µm. The percentage of grains diameter 1.5 µm below, equals 29.7 %. Compared to the sample without ultrasonic vibrations, the sample with it (Figure 8d) has a greater number of grains with a shorter diameter (up to 0.2 µm). The percentage of grains diameter 1.43 µm above, equals 9.95 %.

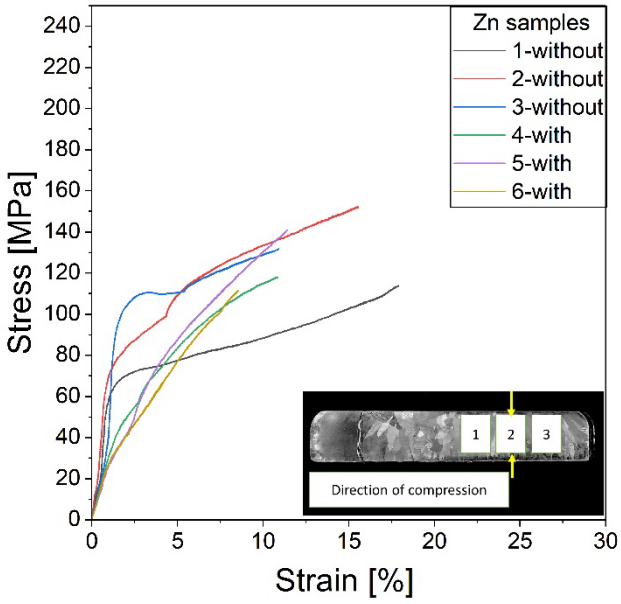

Fig. 9. Compression characteristics for Zn – 2% Bi alloy cast in the traditional and ultrasonic methods. The insert shows how the specimens were cut with the compression direction marked.

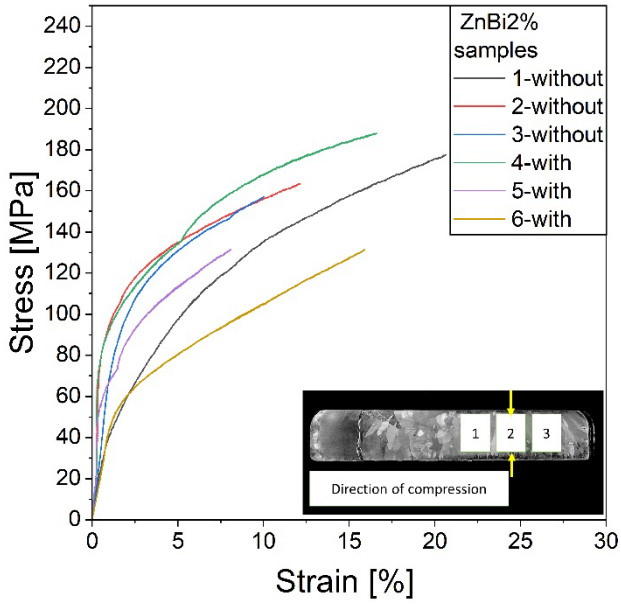

Fig. 10. Compressive test of Zn – 2% Bi samples. Compression characteristics for Zn cast in the traditional and ultrasonic methods. The insert shows how the specimens were cut with the compression direction marked.

The ingot without ultrasonic vibrations (Figure 9) is non–uniform with respect to mechanical properties. The average values of the strength parameters are the following: $Rp_{0.2}$ equals 84.4 MPa, R_m 138.7 MPa and the strengthening coefficient in the plastic range equals 2.9 MPa. As for the ingot cast with the presence of ultrasonic vibrations, the characteristics of the curve is more uniform for all tests. The average values of mechanical properties equals: $Rp_{0.2}$ equals 36.7 MPa, R_m 137.2 MPa and the strengthening factor in the plastic range equals 7.2 MPa. The compression test is done for the Zn – 2 % Bi without ultrasonic vibrations and shows a similar flow for all tests. Average mechanical parameters: $Rp_{0.2}$ equals 86.5 MPa, R_m 138.7 MPa, and the strengthening factor in the plastic range equals 2.8 MPa. As for the Zn – 2% Bi sample with the presence of ultrasonic vibrations (Figure 10), the compression curves are similar in the elastic range but different in the plastic range. The average value of the strength parameters are $Rp_{0.2}$ equals 72.2 MPa, R_m 164.8 MPa, and the strengthening factor in the plastic range equals 4.6 MPa. The data obtained after the compressive test reveal sufficient differences between samples of the two groups. The Zn sample without ultrasonic vibrations has a slight deviation for all examined parameters. An exception is the strengthening factor, which in maximum difference equals 0.9 MPa. In the second examined group, the mechanical parameters are similar in average values, except for the strengthening factor. The strengthening coefficient is higher for the sample with ultrasonic vibrations of about 4.3 MPa. The analogical characteristics of the structure is observed or the Zn – 2% Bi sample with ultrasonic vibrations. The phase of Bi segregates in the Zn matrix according to the ultrasonic vibrations pattern and makes the interfered areas of the sample more visible (Figure 7).

The ultrasonic vibrations create “a sonic lattice” made of nodes from the interference of sonic waves. In this case, the growth of the dendrites is formed in 3 different directions around the casting pit. Its direction is not compatible with the direction of heat dispassion compared to the samples of Zn and Zn – 2% Bi without ultrasonic vibrations. In this group, the ultrasonic vibration is the cause of the distribution and further growth of the grains in the Zn sample. The localization of the sonotrode (Figure 2) generates a vertical wave responsible for the columnar structure of the sample (Figure 4b). The shape of the compression curve is a consequence of the distribution of grains in the Zn sample. Similarly to monocrystal crystallographic orientation, the structure of the ultrasonic-treated sample results in a hard orientation of the grains [18]. For the Zn sample with the presence of ultrasonic vibrations, the microhardness test results (Figure 5) are more even. The maximum properties are higher (min. = 36 HV, max. = 38.8 HV, avg. = 37) than the ones without ultrasonic vibrations. Furthermore, the standard deviation calculated for both samples is almost twice as low for Zn samples without ultrasonic vibrations. The reason for this is the thinner grains of the ingot. In the case of the Zn – 2% Bi without the ultrasonic vibrations, the values between the tests can fluctuate maximally in mechanical parameters cir. 40 MPa in both groups (Zn and Zn – 2%Bi). The difference between both groups is smaller in the case of Zn – 2% Bi samples probably because of the precipitate reinforcement by the Bi phase. Another possible reason for this is the segregation of the Bi precipitation, caused by the direction of heat dissipation (sample without ultrasonic vibrations) or expansion of the network created by ultrasonic vibrations [19].

5. Conclusions

The ultrasonic vibration technologies are commonly used in many aspects such as ultrasonography, sintering, shaping the microstructure of alloy/composites, and casting. Although it was tested in many ways before, the influence on the crystallization process is still not complete. In this paper, ultrasonic vibrations were used as a controlling factor of the crystallization process of a monotectic system. Obtained data indicates a potential of ultrasonic vibrations as a controlling tool for synthesizing a fine macrostructure of a metal matrix, as well as well unified distribution of a secondary phase in alloy. Ultrasonic vibrations were adapted for the casting process by using a crucible implemented to sonotrode. This provides the non-equilibrium conditions of the crystallization process. By fragmentation of the atomic cluster and disturbance in close-range forces, ultrasonic vibration limits the homogeneous nucleation process. As an effect, until the crystallization process reaches the adequate level of free energy, it is withheld. Analysis of the crystallization mechanism under these conditions suggests lowering the crystallization temperature, which will be the target of further research in an extended range of process parameters.

Acknowledgments

The research was supported by project No. 16.16.180.006.

References

[1] Adeleke, A.A., Oki, M., Anyim, I.K., Ikubanni, P.P., Adediran, A.A., Balogun, A.A., Orhadahwe, T.A. Omoniyi, P.O., Olabisi, A.S. & Akinlabi, E.T. (2022). Recent development in casting technology: a pragmatic review. *Journal of Composite and Advanced Materials.* 32(2), 91-102. DOI: 10.18280/rcma.320206.

[2] Karthika, S., Radhakrishnan, T.K. & Kalaichelvi P, (2016). A review of classical and nonclassical nucleation theories. *Crystal Growth & Design.* 16(11), 6663-6681. DOI: 10.1021/acs.cgd.6b00794.

[3] Kelton, K.F. Greer, A.L. (2010). *Nucleation in condensed matter. Applications in materials and biology.* Elsevier.

[4] Qinghua Chen, Ruinan Chen, Jian Su, Qingsong He, Bin Tan, Chao Xu, Xu Huang, Qingwei Dai, & Jian Lu, (2022) The mechanisms of grain growth of Mg alloys: A review, *Journal of Magnesium and Alloys.* 10(9). 2384-2397. https://doi.org/10.1016/j.jma.2022.09.001.

[5] Tammann, G. & Krige, G.J.B. (1925). Die Gleichgewichtsdrucke von Gashydraten. *Zeitschrift für anorganische und allgemeine Chemie.* 146(1), 179-195. https://doi.org/10.1002/zaac.19251460112. (in German).

[6] Jian, X., Xu, H., Meek, T.T., Han, Q. (2005). Effect of power ultrasound on solidification of aluminum A356 alloy. *Materials Letters.* 59(2-3), 190-193. https://doi.org/10.1016/j.matlet.2004.09.027.

[7] Gang Chen, Ming Yang, Yu Jin, Hongming Zhang, Fei Han, Qiang Chen, & Zude Zhao (2019). Ultrasonic assisted squeeze casting of a wrought aluminum alloy. *Journal of Materials Processing Technology.* 266, 19-25. DOI: 10.1016/j.jmatprotec.2018.10.032.

[8] Puga, H., Barbosa, J., Seabra, E., Ribeiro, S. & Prokic, M. (2009). The influence of processing parameters on the ultrasonic degassing of molten AlSi9Cu3 aluminium alloy. *Materials Letters.* 63(9-10), 806-808. DOI: 10.1016/j.matlet.2009.01.009.

[9] Kumar, R., Ansari, Md.S., Mishra, S.S. & Kumar, A. (2014). Effect of ultrasonic mould vibration on microstructure & mechanical properties of pure aluminium casting during solidification. *International Journal of Engineering Research & Technology.* 3(4), 806-808. ISSN: 2278-0181.

[10] Jian, X., Meek, T.T. & Han, Q. (2006). Refinement of eutectic silicon phase of aluminum A356 alloy using high-intensity ultrasonic vibration. *Scripta Materialia.* 54(5), 893-896. DOI: 10.1016/j.scriptamat.2005.11.004.

[11] Chebolu, R., Nallu, R. & Chanamala, R. (2022). Experimental investigation on mechanical behavior of as cast Zn-Al-Cu/SiC/TiB2 hybrid metal matrix composite by ultrasonic assisted stir casting technique. *Engineering Research Express.* 4(2), 025040, 1-9. DOI: 10.1088/2631-8695/ac71f7.

[12] Zhai, W., Liu, H.M. & Wei B. (2015). Liquid phase separation and monotectic structure evolution of ternary Al62.6Sn28.5Cu8.9 immiscible alloy within ultrasonic field. *Materials Letters.* 141, 221-224. DOI: 10.1016/j.matlet.2014.11.087.

[13] Kaukler, W., Fedoseyev, A. (2002). *Report No. NCC8 – 209*. NASA.

[14] Zhao Jiuzhou, & Jiang Hongxiang, (2018). Progress in the solidification of monotectic alloys. *Acta Metallurgia Sinica.* 54(5), 682-700. DOI: 10.11900/0412.1961.2018.00080

[15] Nad, M., Cicmancova, L. (2012). The effect of the shape parameters on modal properties of ultrasonic horn design for ultrasonic assisted machining. In 8th International Daam Baltic Conference Industrial Engineering, 19-21 April 2012 (pp. 57-62). Tallinn, Estonia.

[16] Karthikeyan, P. & Pramanik, S. (2018). Effect of vibration of moulding on the gravity casted specimen during pouring of molten aluminium in metallic mould. Materials Science and Engineering. *IOP Conference Series: Materials Science and Engineering*. 402 012037, 1-9. DOI: 10.1088/1757-899X/402/1/012037.

[17] Nagasivamuni, B., Wang, G., StJohn, D.H. & Dargusch, M.S. (2018). The effect of ultrasonic treatment on the mechanisms of grain formation of ascast high purity zinc, *Journal of Crystal Growth.* 495, 20-28. DOI: doi.org/10.1016/j.jcrysgro.2018.05.006.

[18] Kurgan, A. & Madej, Ł. (2023). Role of crystallographic orientation in material behaviour under nanoindentation: Molecular Dynamics study. *Material Science-Poland*. 41(3), 18-26. DOI:10.2478/msp-2023-0032.

[19] Wei Zhai, Hanman Liu, Pengfei Zuo, Xiannian Zhu Bingbo Wein, (2015). Effect of power ultrasound on microstructural characteristics and mechanical properties of Al81.3Sn12.3Cu6.4 monotectic alloy. *Progress in Natural Science: Materials International.* 25(5), 471-477. https://doi.org/10.1016/j.pnsc.2015.10.006.